THE JOURNAL OF BIOLOGICAL CHEMISTRY VOL. 286, NO. 23, pp. 20977–20990, June 10, 2011
Printed in the U.S.A.

A Novel Specificity Protein 1 (*SP1*)-like Gene Regulating Protein Kinase C-1 (Pkc1)-dependent Cell Wall Integrity and Virulence Factors in *Cryptococcus neoformans*[*][S]

Received for publication, February 11, 2011, and in revised form, April 8, 2011 Published, JBC Papers in Press, April 12, 2011, DOI 10.1074/jbc.M111.230268

Amos Adler[‡§], Yoon-Dong Park[¶], Peter Larsen[‖], Vijayaraj Nagarajan[**], Kurt Wollenberg[**], Jin Qiu[¶], Timothy G. Myers[‡‡], and Peter R. Williamson[§¶1]

From the [‡]Section of Pediatric Infectious Disease, Department of Pediatrics, University of Chicago, Chicago, Illinois 60637, the [§]Section of Infectious Diseases, Department of Medicine, University of Illinois College of Medicine, Chicago, Illinois 60612, the [¶]Laboratory of Clinical Infectious Diseases, the [**]Bioinformatics and Computational Biosciences Branch, Office of Cyber Infrastructure and Computational Biology, and the [‡‡]Genomic Technologies Section, Research Technologies Branch, NIAID, National Institutes of Health, Bethesda, Maryland 20892, and the [‖]Biosciences Division, Argonne National Laboratory, Lemont, Illinois 60439

Eukaryotic cells utilize complex signaling systems to detect their environments, responding and adapting as new conditions arise during evolution. The basidiomycete fungus *Cryptococcus neoformans* is a leading cause of AIDS-related death worldwide and utilizes the calcineurin and protein kinase C-1 (Pkc1) signaling pathways for host adaptation and expression of virulence. In the present studies, a C-terminal zinc finger transcription factor, homologous both to the calcineurin-responsive zinc fingers (Crz1) of ascomycetes and to the Pkc1-dependent specificity protein-1 (Sp1) transcription factors of metazoans, was identified and named *SP1* because of its greater similarity to the metazoan factors. Structurally, the *Cryptococcus neoformans* Sp1 (Cn Sp1) protein was found to have acquired an additional zinc finger motif from that of Crz1 and showed Pkc1-dependent phosphorylation, nuclear localization, and whole genome epistatic associations under starvation conditions. Transcriptional targets of Cn Sp1 shared functional similarities with Crz1 factors, such as cell wall synthesis, but gained the regulation of processes involved in carbohydrate metabolism, including trehalose metabolism, and lost others, such as the induction of autophagy. In addition, overexpression of Cn Sp1 in a *pkc1*Δ mutant showed restoration of altered phenotypes involved in virulence, including cell wall stability, nitrosative stress, and extracellular capsule production. Cn Sp1 was also found to be important for virulence of the fungus using a mouse model. In summary, these data suggest an evolutionary shift in C-terminal zinc finger proteins during fungal evolution, transforming them from calcineurin-dependent to *PKC1*-dependent transcription factors, helping to shape the role of fungal pathogenesis of *C. neoformans*.

The basidiomycete yeast *Cryptococcus neoformans* has emerged as one of the major causative agents of meningoencephalitis in immunocompromised hosts, such as persons with AIDS, organ transplant recipients, and patients receiving high doses of corticosteroid treatment. Systemic infections can also occur in immunocompetent individuals (1, 2). As rates of infection have diminished in developed countries, attention is increasingly being focused on the high rates of cryptococcosis in the developing countries of Africa and Asia, where cryptococcosis has been found to account for an estimated 17% of AIDS-related deaths (3). Recent studies have shown cryptococcosis to account for over 600,000 deaths annually, resulting in a disease burden worldwide approaching that of tuberculosis (4).

The three best known virulence-associated traits of *C. neoformans* include its ability to grow at 37 °C (5), the presence of a copper-containing laccase that is capable of producing melanin pigments (6), and a high M_r polysaccharide capsule (7–9). Although temperature and capsule are likely to have multiple structural genes involved in expression, melanin production has been shown to be dependent on two laccase enzymes encoded by *LAC1* and *LAC2*, the former of which is the predominant enzyme under pathogenic conditions (6), making *LAC1* an excellent maker for studying virulence regulation in *C. neoformans*.

Yeast cells, including *C. neoformans*, are continuously exposed to a wide variety of environmental stresses in both their natural habitats and their resident hosts. These stresses include changes in temperature, osmolarity, pH, nutrients, and exposure to reactive oxygen and nitrogen molecules. They subsequently sense and react to these changes through a complex network of signal transduction pathways, thus adapting to their surroundings and ensuring repair of cellular damage. A major cellular pathway mediating these responses is the protein kinase C (*PKC1*) pathway. Within this pathway, activation of Pkc1 leads to sequential phosphorylation of a mitogen-activating protein kinase (MAPK) cascade, consisting of Bck1p, two redundant MAPK kinases (Mkk1p and Mkk2p), and the MAPK, Slt2/Mpklp (10). In *Saccharomyces cerevisiae*, Rlm1p (11–14) and Swi4/Swi6 (15) are the main transcription factors

[*] This work was supported, in whole or in part, by National Institutes of Health Grants AI45995 and AI49371 and by the Intramural Research Program of the National Institutes of Health, NIAID.

[S] The on-line version of this article (available at http://www.jbc.org) contains supplemental Methods and supplemental Table S1 and Figs. S1–S8.

[1] To whom correspondence should be addressed: 9000 Rockville Pike, Bldg. 10, Rm. 11N234, MSC 1888, Bethesda, MD 20892. Fax: 301-480-7321; E-mail: williamsonpr@mail.nih.gov.

(TFs)[2] responsible for Slt2/Mpklp cell wall regulation. At least 25 genes that are involved in the biosynthesis of the cell wall and are regulated by Slt2/Mpklp and Rlm1p have been described (11).

In *C. neoformans*, mutation of *PKC1* results in mutants that have profound cell wall integrity defects, including an inability to grow without the addition of an osmotic stabilizer, such as sorbitol, and profound growth defects in the presence of various stressors. In addition, major virulence factors are altered in *pkc1*Δ strains, including an inability to grow in 37 °C, aberrant capsule, and decreased melaninogenesis (16). The phenotypic features of mutants of the major genes regulated by the Pkc1 pathway have also been characterized in *C. neoformans*, including Bck1, Mkk2, and Mpk1 (16–17). However, although Pkc1 has been implicated in resistance to nitrosative stress and laccase expression, the transcription factor(s) responsible for the signal from Pkc1 has not been identified.

In the present studies, we sought to characterize a C-terminal zinc finger C2H2 type transcription factor protein, annotated *CNAG_00156* (Broad Institute Web site; NCBI annotation XP_566613.1), that was first thought to represent a calcineurin-dependent zinc finger protein (Crz1), based on close homology to the *S. cerevisiae* and *Candida albicans* Crz1 homolog sequence. These studies were motivated by a previously described role for the Ca^{2+}-activated calcineurin pathway in cryptococcal virulence (5) and a role for calcium activation of laccase (18) as well as enzyme inhibition by the calcineurin inhibitor, FK506.[3] However, to our surprise, we could not find evidence that *CNAG_00156* was part of the calcineurin pathway. Further studies to identify the relevant signal transduction pathway utilized a novel transcriptional clustering screen that identified Pkc1 as a likely signaling pathway for *CNAG_00156*. Biochemical and epistatic studies provided additional evidence linking the Pkc1 signal transduction pathway and the cryptococcal zinc finger transcription factor.

EXPERIMENTAL PROCEDURES

Strains, Plasmids, and Media—Strains used in this study are detailed in supplemental Table S1. All strains were grown on YPD medium (1% yeast extract, 2% Bacto-peptone, and 2% dextrose). Solid media contained 2% Bacto-agar. All *PKC1* deletion strains were grown on YPD supplemented with 1 M sorbitol. Glucose starvation experiments were done as described previously (19). Selective media included either YPD containing 100 units/ml hygromycin B (InvivoGen) or asparagine minimal medium as described previously (20). A modified Bluescript SK vector (Stratagene) with the 2.4-kb hygromycin B resistance gene under the control of a cryptococcal Actprmtr (21) was a gift of G. Cox (Duke University, Durham, NC). In addition to the cryptococcal shuttle vector pORA-KUT (19), a hygromycin B-containing vector was generated by replacing the *URA5* transformation marker with the hygromycin B resistance gene at the KpnI site, generating pORA-KUT (HygB).

Sequence Data Mining and Analysis—Sequence data were retrieved from the NCBI, Broad Institute Web site, and the *Saccharomyces* Genome Database, for *Homo sapiens*, *C. neoformans*, and *S. cerevisiae*, respectively. For the analysis of metazoan and fungal zinc finger motifs, sequences were retrieved using BLASTp searches with human Sp1 and *C. neoformans* CNAG_00156 as the query sequences. Occasionally there were BLASTp hits to multiple zinc finger motifs in target sequences. For these cases, the highest scoring hit was used as the putative homolog. The full protein sequences were aligned using MUSCLE (22), and the zinc finger motifs were manually extracted and aligned. A phylogenetic analysis of the zinc finger motifs (supplemental Fig. S3*b*) was performed using the heuristic parsimony algorithm of PAUP 4b10 (23). To evaluate support for the groups in the tree, 500 nonparametric bootstrap replicates were analyzed. PAUP returned 500 equally parsimonious trees for which the 50% majority rule consensus is shown. In Fig. 2*B*, clades consisting of major taxonomic groups from supplemental Fig. S3*b* were collapsed when possible. All of the variation among the equally parsimonious trees occurred within these collapsed groups, so the branches shown in the figure were found in all 500 trees.

*Generation of Cn sp1*Δ *and Cn sp1*Δ*::Cn SP1 Strains*—Standard methods were used for disruption and complementation of the Cn *SP1* (*CNAG_00156*) gene, as described previously (20). Briefly, to make the deletion construct, two PCR-amplified fragments of the Cn *SP1* homolog (using primers Crz1 S1 XbaI (5′-GCTCTAGAATGGCAGATCCAGCCTCAC) plus Crz1 500 A EcoRI (5′-GGAATTCTGTTCGGACATCCTGCCTTC) and Crz1 3171 S BglII (5′-GAAGATCTCACAAGGCATTTTAATCTCAAGG) plus and Crz1 3693 A XhoI (5′-CCGCTCGAGAATCCTCTTCACTCGTTTCACTC)), the first amplified fragment digested with XbaI and EcoRI and the second digested with BglII and XhoI, were mixed with a 1.4-kb PCR fragment of the *URA5* gene described previously (20), digested with BglII and EcoRI, and ligated to BlueScript SK digested with XbaI and XhoI. The final disruption allele with a 1.3-kb *URA5* marker flanked on either side by a 500-bp DNA sequence homologous to genomic regions of the Cn *SP1* gene was PCR-amplified and introduced into H99 *ura5* cells via a biolistic approach (21) to effect a 3.7-kb deletion within the Cn *SP1* coding region. Transformants were screened for a potential Cn *SP1* deletion mutant by a PCR approach, and the specific disruption of the Cn *SP1* gene in candidate mutants was verified by Southern blot analysis and PCR of cDNA, to verify the lack of Cn *SP1* transcription (supplemental Fig. S7). To complement the Cn *sp1*Δ mutant strain, a 5.7-kb genomic fragment encompassing the full ORF of Cn *SP1* plus ~1500 bp of the 5′ promoter region and 500 bp of the 3′-UTR was PCR-amplified using a primer set of Crz1 US-1500 BamHI (5′-GCGGATCCATACACGACAAACACATCGCTACA) and Crz1-500 3′UTR-A-BamHI (5′-CGCGGATCCACGAT GAAAATGAAGGCTTCGACAATA) and then cloned into the modified pBluescript SK vector containing the hygromycin B resistance gene to generate the complementation construct, which was introduced into Cn *sp1*Δ mutant cells by a biolistic approach. Transformants were selected on hygromycin-containing YPD

[2] The abbreviations used are: TF, transcription factor; MIC, minimum inhibitory sensitivity; Cn, *C. neoformans*; Ab, antibody.
[3] S. S. Zhang and P. R. Williamson, unpublished observation.

agar plates. Genomic insertion of the WT Cn *SP1* construct in the complement was verified by uncut Southern blot.

Generation of Constituent Expression and GFP-tagged Strains of PKC1 and Cn SP1—Because the Cn *SP1* and *PKC1* genes contain an EcoRI site, cloning into the pORA-KUT vector required additional restriction sites. An oligonucleotide polylinker containing the restriction sites BglII-BamHI-XbaI-NarI-NheI-end codon-EcoRI was inserted between the BglII and EcoRI sites of pORA-KUT. The ~730-bp *C. neoformans* Actprmtr (with or without a c-*myc* tag) was amplified from H99 DNA using the primer Actprmtr 1S BglII (5′-GGAAGATCT-TGTCGGAGGAGAGGATGATGGTAAC), Actprmtr 730A BamHI (5′-CGCGGATCCGTTGGGCGAGTTTACTAATG-GAAAAAGA), or Actprmtr0A-Myc-BamHI (5′-CGCGGAT-CCGAGGTCCTCCTCGGAGATGAGCTTCTGCTCCATG-TTGGGCGAGTTTACTAATGGAAAAAG), cut with BglII and BamHI, and inserted into the BamHI site, obliterating its 5′-end, generating pORA-KUT-pACT. *PKC1* and Cn *SP1* constituent expression vectors were generated by inserting the coding region after the Actprmtr (including the c-*myc* tag in the Cn *SP1* insert). The *PKC1* coding region was amplified using primers PKC 1S BamHI (5′-CGGGATCCATGGTGCGTGG-ATATCTGCCA) and PKC 3784A NheI (5′-CTAGCTAGCC-TAGGCTTGTGCTGCAGCCCA). The Cn *SP1* coding region was amplified using primers Crz1–1S-BamHI (5′-CGGGATC-CATGGCAGATCCAGCCTCAC) and Crz1 A3695 NheI (5′-CTAGCTAGCTTAATCCTCTTCACTCGTTTCACTC). Inserts were cut with BamHI and NheI and ligated into the corresponding restriction sites in pORA-KUT-pACT, generating pORA-KUT-pACT-Cn SP1 and pORA-KUT-pACT-PKC1. A *C. neoformans* codon-adjusted GFP fragment was amplified from a previously constructed plasmid (24) by using primers GFP 1S BglII (5′-GGAAGATCTATGTCCAAGGGTGAGGA-GCTC) and GFP 741A BamHI (5′-CGGGATCCCTCGGCGG-CGGCGG). The insert was cut with BamHI and BglII and inserted in the BamHI of pORA-KUT-pACT-Cn SP1, positioning the GFP on the 5′ end of the coding region, generating pORA-KUT-pACT-GFP-Cn SP1. The vectors were linearized with I-SceI and transformed by electroporation as described previously (24) as follows: pORA-KUT-pACT-PKC1 into Cn *sp1*Δ (Cn *sp1*Δ::pACT-*PKC1*); pORA-KUT-pACT-Cn SP1 (including the c-*myc* tag) into Cn *sp1*Δ, *cna1*Δ, and *pkc1*Δ (Cn *sp1*Δ::pACT-Cn *SP1*, *cna1*Δ::pACT-Cn *SP1*, and *pkc1*Δ::pACT-Cn *SP1*, respectively); and pORA-KUT-pACT-GFP-Cn SP1 into Cn *sp1*Δ (Cn *sp1*Δ::GFP-Cn *SP1*). Transformants were selected on hygromycin B and verified by sequencing. Constituent expression was tested by quantitative RT-PCR and by Western blot. Functionality of the c-*myc*-tagged Cn *SP1* was verified by reversal of the Cn *sp1*Δ mutant cell wall defects (Fig. 4).

Cell Wall Integrity Assays—Strains were grown on YPD plus 1 M sorbitol plates for 2 days at 30 °C. Then they were suspended in PBS to an A_{600} of 0.1 and underwent 5-fold serial dilutions in PBS. 10 μl of each dilution was applied to YPD; YPD + 1 M sorbitol at 30 and 37 °C; YPD + 1 M sorbitol with the following: 0.5 mg/ml calcofluor white (Fluorescent Brightener 28, Sigma), 0.5% Congo red (Sigma), 0.01% SDS, 200 mM $CaCl_2$, 50 mM $LiCl_2$, 100 μM EDTA, and 1 mM $NaNO_2$. Plates were incubated for 2 days at 30 °C.

Caspofungin Susceptibility Testing—Due to the extreme fastidiousness of the *pkc1*Δ strain, we were not able to test minimum inhibitory sensitivities (MICs) with standard broth microdilution techniques; hence, we designed a specialized agar dilution assay. Cells were grown as described above and were suspended in PBS to an A_{600} of 0.132. Cell suspensions were diluted 1:222, and 20 μl of each strain were spotted on YPD + 1 M sorbitol agar plates with caspofungin concentrations from 0.25 to 16 mg/liter, including a no-drug control plate. Plates were observed for 48 h, and the MIC was determined at the point of visible growth.

Virulence Factor Expression and Virulence Studies—For measuring capsule formation under non-inducing conditions, cells were grown overnight on YPD + sorbitol media, stained with India ink, and observed under microscopy. Laccase activity was assessed as described previously (25). Virulence studies were conducted according to a protocol using a previously described mouse meningoencephalitis model, with five mice in each group (19). Animal studies were approved by the University of Illinois at Chicago Animal Care Committee.

Microarray Experiments—Cn Sp1 comparative screening by a *C. neoformans* glass microarray (Fig. 1) was as follows. For the comparative transcriptional profile experiment, H99, Cn *sp1*Δ, *pkc1*Δ, *cna1*Δ, *pka1*Δ, *ssa1*Δ, *vad1*Δ, *ste12*Δ, and *bck1*Δ strains were grown overnight in YPD (with 1 M sorbitol in *pkc1*Δ) in 30 °C shaker incubator to a mid-log phase and then induced by glucose starvation for 1 h. RNA was extracted and purified; cDNA was prepared, labeled, and hybridized to H99 glass microarray slides; and the slides were scanned and analyzed as described previously (26, 27). Feature signal was corrected for local background. Significance of signal was calculated as the two-tailed *p* value of a *z*-test for all replicate features, using the S.D. value of all measured features on the array. *p* values were corrected for false discovery rate using the Benjamini-Hochberg method (28). Clustering of signal intensities was then performed in "Expression profiler" (see the EPCLUST Web site) with correlation measure-based distance and average linkage.

Quantitative RT-PCR Experiments—*C. neoformans* strains were grown to a mid-log phase prior to induction. RNA was extracted before and following induction and treated with the RNase-free DNase Set (Qiagen). 5 μg of total RNA were used for cDNA generation using Invitrogen SuperScript® II reverse transcriptase and oligo(dT) primers in a 30-μl reaction mix. cDNA (1 μl) was used as a template for real-time reactions containing primer sets and iQ™ SYBR® Green Supermix (Bio-Rad). The following primers were used in the epistasis studies: for Cn *SP1*, Crz1 qRT2939S (5′-GTTGTCCCAAAGCTATC-GTCG) and Crz1 qRT3055A (5′-GACGAGCAAACTTCTTC-CCACA); for *PKC1*, PKC cDNA 2225S (5′-CCAACAACAAG-TGACGCAGAG) and PKC RT 2300A (5′-TTACCCTTACC-CAGCACTGCTAA); for *ACT1*, actin qRT 1200S (5′-ATGTA-CAATGGTATTGCCGACCGTATG) and actin qRT 1455A (5′-GCTCTTCGCGATCCACATCTG) (microarray validation study primers are not shown). Quantitative PCR data were analyzed with Bio-Rad iQ5 software, and results are presented either as relative expression (Δ*Ct*) with *ACT1* as control (epis-

tasis studies) (29) or as normalized expression ($\Delta\Delta Ct$) for the microarray validation studies.

Immunoprecipitation and Western Blotting—Cultures were grown overnight in YPD or in YPD containing 1 M sorbitol (150 ml) for the *pkc1*Δ strain at 30 °C with shaking to mid-log phase and then induced with either 10 μg/ml calcofluor white, 1 mM $NaNO_2$, or glucose starvation for 1 h. Cells were lysed using glass beads with phenylmethylsulfonyl fluoride (final concentration of ~1 mM) and Halt® protease and phosphatase inhibitor mixture (Pierce) and eluted with the immunoprecipitation lysis/wash buffer taken from the Pierce Classic IP kit (Pierce). The protein extract was adjusted to a final concentration of 1 mg/ml (2 mg/ml was used for *pkc1*Δ::pACT-Cn *SP1*). 700 μl of protein extract were mixed with 5 μl of monoclonal anti-c-*myc* antibody produced in mice (Sigma-Aldrich) and were incubated with rotation in 4 °C for 4 h. Immunoprecipitation was then carried out with the Pierce Classic IP kit following the manufacturer's instructions. From a final eluent volume of 50 μl of immunoprecipitated Cn Sp1, 30 μl were loaded for the anti-phosphorylated Cn Sp1 experiment, and 20 μl were run as loading control, using 7.5% SDS-PAGE. Gels were transferred overnight to a PVDF membrane and blocked with Invitrogen membrane blocking solution. Primary antibody blot was done with either the Invitrogen phosphoprotein antibody sampler pack at a final concentration of each antibody (anti- phosphorylated serine, threonine, and tyrosine) of 1 μg/ml to detect phosphorylated residues on Cn Sp1 or the anti c-*myc* antibody (1:1000) to detect total c-*myc*-tagged Cn Sp1. Secondary antibody blot was done with Pierce anti-rabbit HRP diluted 1:3000 and Pierce anti-mouse HRP diluted 1:5000 (phosphorylated Cn Sp1 experiment) or Pierce anti-mouse HRP diluted 1:2500 (total Cn Sp1 experiment). Signal detection was done with the Pierce SuperSignal according to the manufacturer's directions.

Chromatin Immunoprecipitation (ChIP)—ChIP was performed as described previously (30) with the following modifications. Following induction, formaldehyde was added to a final concentration of 1%, and incubation was continued at room temperature for 30 min. Cross-linking was quenched with glycine (8.5 ml of 2.5 M to ~160 ml of culture) at room temperature for 5 min. Cells were harvested, washed three times in cold PBS, and lysed with glass bead beating. Cell extract was sonicated to produce an average size of ~750 bp. The extract was centrifuged, and supernatant was mixed with either 5 μl of anti-c-*myc* or mouse IgG1 as an isotype control. Immunoprecipitation was performed as described above, except that elution was done with several washes of elution buffer (50 mM Tris-HCl, pH 8.0, 10 mM EDTA, 1% SDS), up to a total volume of 300 μl. DNA enrichment of promoter regions in the ChIP eluent was assayed by quantitative PCR as described above, with the following primers. The *ACT1* genomic region was used as a control with the primers actin RT 739S (5′-ACCACTTCTGCCGAGCGAGA) and actin RT 945A (5′-GAGACCAAGGAGAGAAGGCTGG). The malate dehydrogenase promoter region at −170 to 0 bp from the ORF was used with primers pMDH 1396S (5′-CGAGTCGTAAACAACAGAATGGTC) and pMDH 1576A (5′-TACGGGTCATTCTGGGCTGG). The 1,4-α-glucan-branching enzyme promoter region at −291 to −40 from the ORF was used with primers α-glucan promoter RT 1009S (5′-CGAAAGCGGCAAGTCAGGTG) and α-glucan promoter RT 1063A (5′-GACTGAAGACGAGAAATGAGAAGGGA). The *HSP12* promoter region at −300 to −210 from the ORF was used with primers *HSP12* promoter RT S (5′-GCAGCAACACAAGCAGCAA) and *HSP12* promoter RT A (5′-CGGCAAGAACCAGCAACAG). Promoter occupancy by Cn Sp1 was expressed as a ratio of the target promoter signal immunoprecipitated to the c-*myc* antibody *versus* the isotype control; the ratio in the *ACT1* genomic region was used as a control.

Fluorescent Microscopy of GFP-tagged Cn Sp1—Cells were grown overnight to a mid-log phase prior to induction as described above. At each time point, slides were prepared with DAPI and observed under fluorescent microscopy as described (31). Triplicates of 100 cells each were observed for nuclear localization and expressed as mean ± S.D.

Statistics—Statistical significance of mouse survival times was assessed by Kruskall-Wallis analysis (analysis of variance on rank sum test). Statistical analysis was conducted using GraphPad Prism software, version 4.03.

RESULTS

CNAG_00156 Is Not a Functional Homolog of Yeast CRZ1 Despite Sequence Similarity—We identified *CNAG_00156* as a potential homolog of the *S. cerevisiae* calcineurin-responsive transcription factor (Crz1), based on highest similarity (58.7%) to the ascomycete factor. However, during our study, this hypothesis appeared unlikely, based on three lines of evidence: 1) lack of restoration of temperature-dependent or cell wall-defective phenotypes after overexpression of *CNAG_00156* in *cna1*Δ (*cna1*Δ::pACT-Cn *SP1*) (supplemental Fig. S1*A*); 2) lack of a calcineurin-dependent size shift of the CNAG_00156 protein on SDS-polyacrylamide gel, suggesting a lack of calcineurin-dependent post-translational modifications (supplemental Fig. S1*C*) (32, 33); 3) lack of calcium-dependent nuclear translocation of a GFP-tagged *CNAG_00156* (supplemental Fig. S1*D*) previously demonstrated with Crz1 homologs (32, 33).

*Transcriptional Profiling Reveals That cnag_00156*Δ *and pkc1*Δ *Mutant Strains Share Similar Transcriptional Profiles under Starvation Conditions*—To elucidate the potential cellular pathway related to *CNAG_00156*, we compared the transcriptional profile of *cnag_00156*Δ with knock-out mutants of genes involved in laccase production, *pka1*Δ, *pkc1*Δ, *ssa1*Δ, and *vad1*Δ, as well as genes related to pathways with a known C-terminal zinc finger transcription factor in *S. cerevisiae*: *cbk1*Δ (RAM pathway) and *cna1*Δ. An *ssa1*Δ mutant in an H99 background was constructed for these studies and is described in the supplemental Methods (supplemental Fig. S7). The *ste12*Δ mutant, which has wild type virulence and laccase expression in the H99 background (34), was chosen as an outgroup control. Because nutrient starvation is a condition required for induction of numerous virulence-associated cellular programs, such as autophagy (20) and laccase expression (35), glucose starvation conditions were chosen for the strain comparisons.

Compared with the other mutants, the *pkc1*Δ strain exhibited the transcriptional profile most similar to that of *cnag_00156*Δ (Fig. 1, *A* and *B*, and supplemental Fig. S2), with 48 shared down-regulated genes (of 208 and 194 down-regu-

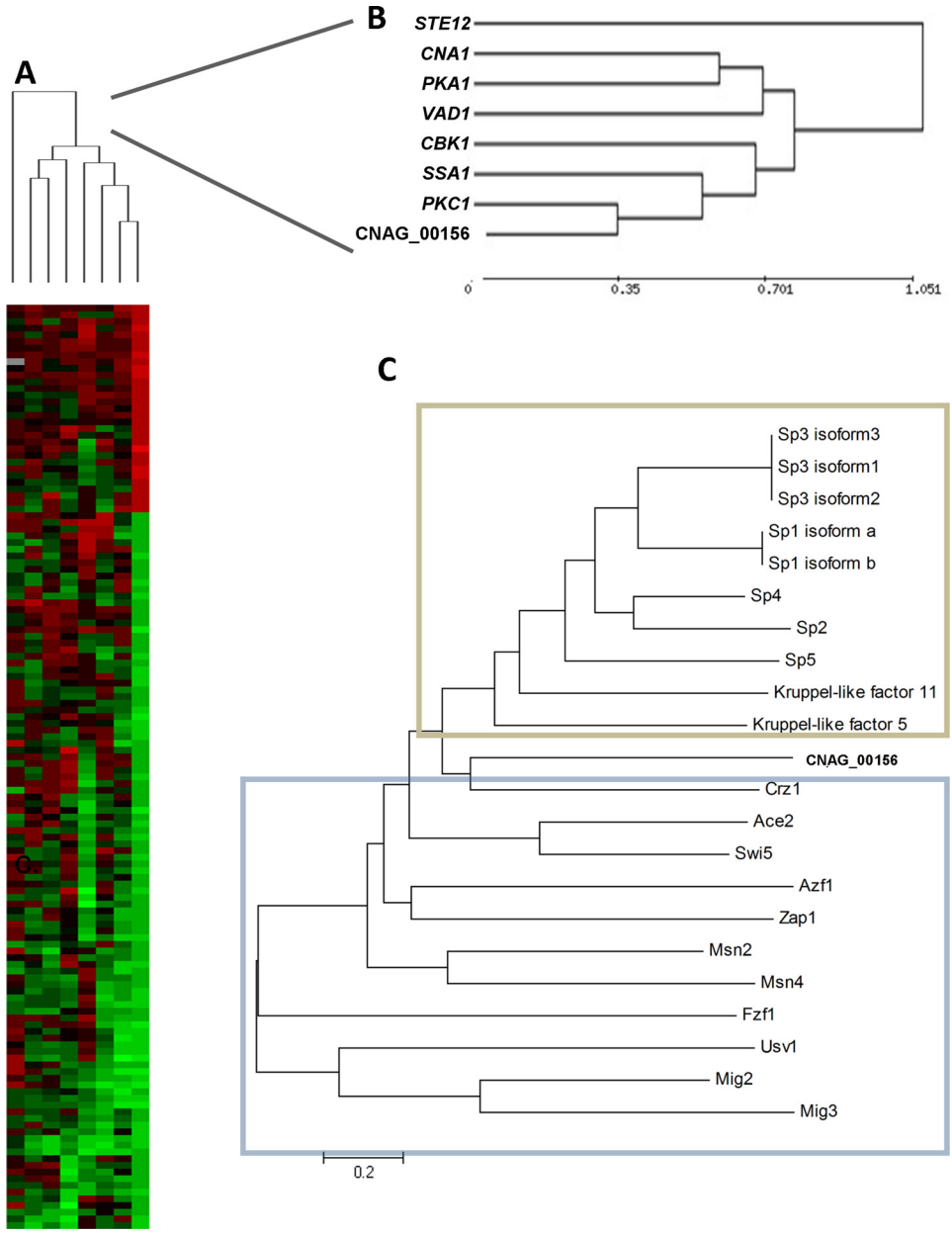

FIGURE 1. **Transcriptional and protein sequence comparison of a C-terminal zinc finger (*CNAG_00156*).** *A*, heat map display of a comparative microarray experiment of *C. neoformans* strains Cn *sp1*Δ (*cnag_00156*Δ), *pkc1*Δ, *pka1*Δ, *cna1*Δ, *cbk1*Δ, *ssa1*Δ, *ste12*Δ, and *vad1*Δ. Strains were grown overnight to mid-log phase and induced in 0% glucose medium for 1 h before RNA extraction. WT (H99) induced under the same conditions was used as reference for each mutant. A cluster analysis of genes significantly altered in mutant strains with $p < 0.0001$ is presented. *B*, *close-up view* of the cluster analysis presented in *A*. *C*, neighbor-joining phylogenic analysis of the Cn Sp1 (Cnag_00156) with *S. cerevisiae* (*blue frame*) and *H. sapiens* (*tan frame*) C-terminal zinc finger transcription factors.

lated genes in *cnag_00156*Δ and *pkc1*Δ, respectively), supporting a possible common pathway. Validation of sample genes from the microarray experiment was performed by Northern blot (supplemental Fig. S4) and quantitative RT-PCR studies (supplemental Fig. S5) and will be described in further detail elsewhere.

CNAG_00156 Shares Homology to C-terminal Zinc Finger Transcription Factors in S. cerevisiae and H. sapiens—Comparison of the full-length putative amino acid sequence of *CNAG_00156* with other known C-terminal zinc finger TFs of *S. cerevisiae* failed to identify homologous yeast zinc finger proteins (Fig. 1*C*, *blue frame*) known to be related to Pkc1. Indeed, the known *PKC1*-related TFs in *S. cerevisiae*, Rlm1 and Swi4, are not C-terminal zinc finger proteins. In contrast, metazoans, represented by mammalian (*H. sapiens*) cells (Fig. 1*C*, *tan frame*) express several *CNAG_00156* homologs with homology to the Sp TF family (58.7 and 54.5% similarity with Crz1 and Sp1, respectively). Interestingly, within the Sp TF family, Sp1 and Sp3 are known to be regulated by Pkc1 (36, 37). Based on this homology, we decided to designate *CNAG_00156* as *C. neoformans SP1* (Cn *SP1*).

Structural Analysis of Cn Sp1, H. sapiens Sp1, and S. cerevisiae Crz1—To better understand the structural relationship between Cn Sp1 and metazoan Sp1, we compared the zinc fin-

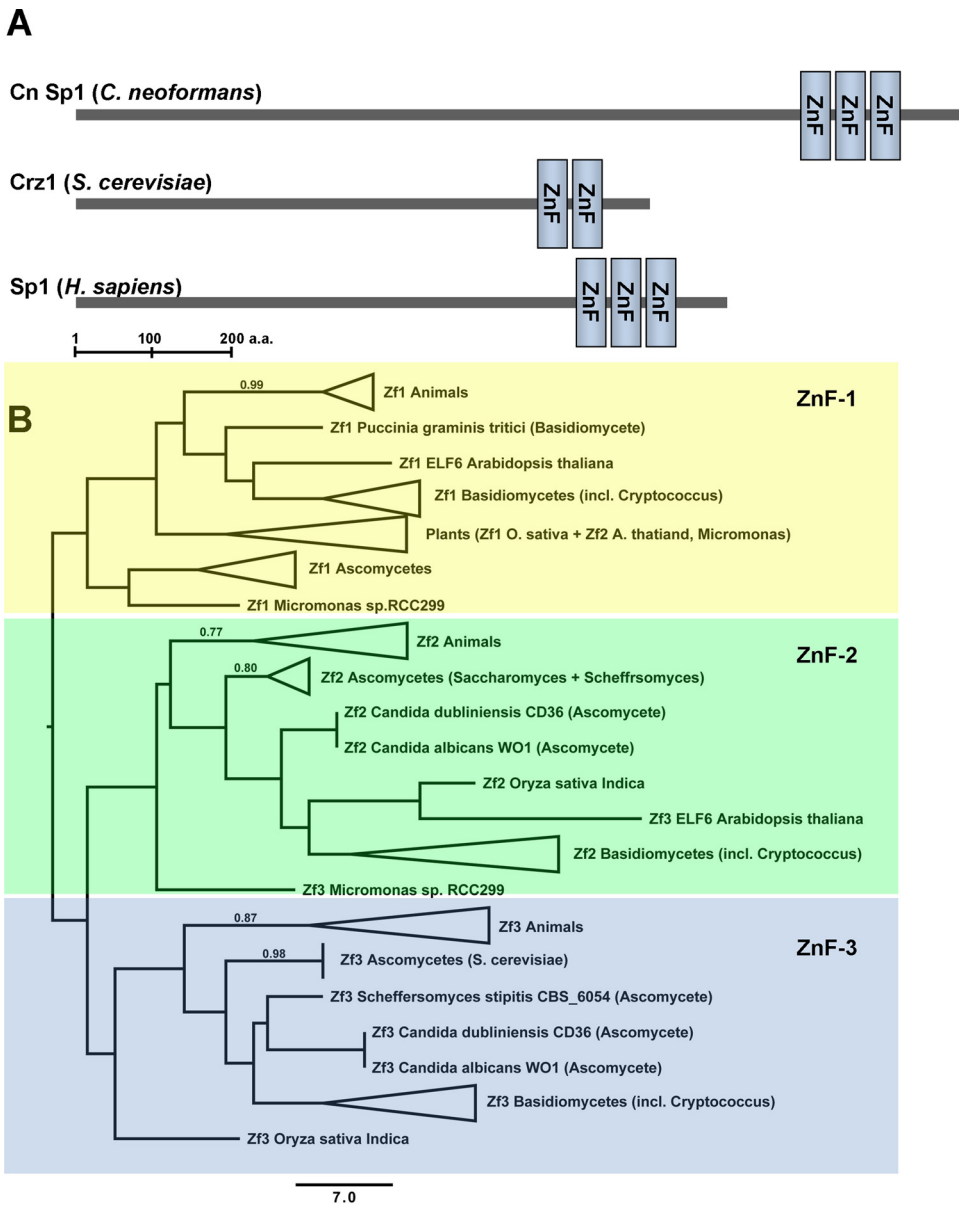

FIGURE 2. ***C. neoformans* and the *H. sapiens* Sp1 share similar functional domains.** *A*, the SMART-identified zinc finger domain pattern, showing Cn Sp1, Crz1, and *H. sapiens* Sp1 zinc finger domains (*ZnF*). *B*, phylogenetic analysis of metazoan and fungal zinc finger motifs (*ZnF-1* to *-3*) of *C. neoformans*. Parsimonious trees were constructed using the heuristic parsimony algorithm of PAUP 4b10, as described under "Experimental Procedures." Clades consisting of major taxonomic groups were collapsed when possible. Bootstrap support percentages greater than 70% are shown *above* the *branches*.

ger elements of Cn Sp1 with those of the *S. cerevisiae* Crz1 and the archetype *H. sapiens* Sp1 because this region of the protein is the most highly conserved across species and is an important functional motif. SMART analysis (38) showed that the distribution of the C-terminal zinc finger domains were of a similar pattern in both Cn Sp1 and *H. sapiens* Sp1 (Fig. 2*A*), with three domains in Cn Sp1 (944–968, 974–1001, and 1007–1034) and *H. sapiens* Sp1 (626–650, 656–680, and 686–708) and only two domains (569–591 and 597–619) in Crz1 from *S. cerevisiae*. This is an important divergence because the zinc finger domain is the principal DNA-binding element within these classes of transcription factors (39, 40).

Phylogenetic analysis of homologous C-terminal zinc finger domains across selected fungi and metazoans revealed further sequence divergence between the basidiomycete factor and those of ascomycetes, such as Crz1 (Fig. 2*B* and supplemental Fig. S3*A*). Interestingly, the first zinc finger domain of basidiomycete fungi, such as *C. neoformans*, appears to cluster best with metazoans rather than ascomycete yeast, such as *S. cerevisiae*, although the relationship was weakly supported due to the short sequences of the motif. In contrast, the second zinc finger motif appears to follow classic evolutionary relationships with basidiomycete fungi clustering with the ascomycete motif. The third zinc finger motif of *C. neoformans* fulfills the protein family definition of a zinc finger motif ($CX_{1-5}CX_{12}HX_{3-6}$(H/C)) (41), similar to the metazoan zinc finger motifs (supplemental Fig. S3*B*). However, a previously undescribed motif bearing a resemblance to zinc finger domains was also found in the *S. cerevisiae* Crz1 factor. A 9-amino acid insertion between the first two cysteine residues results in its failure to be classified as

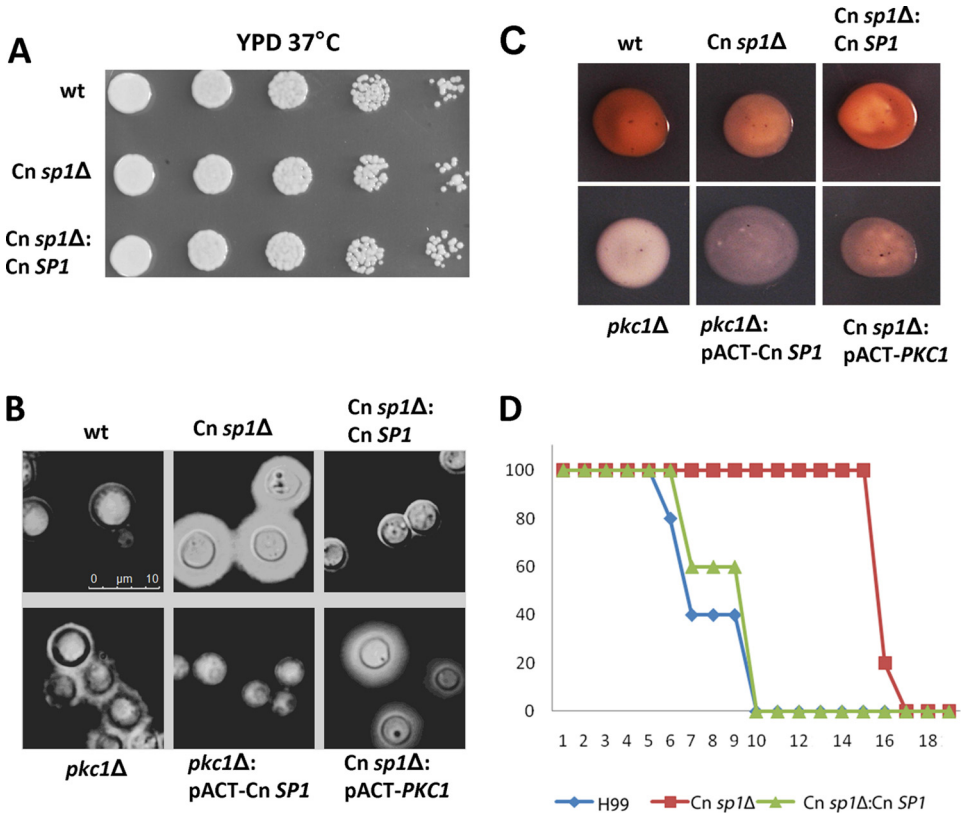

FIGURE 3. **Cn *sp1*Δ and *pkc1*Δ have altered virulence factors.** *A*, WT (H99), Cn *sp1*Δ, and Cn *sp1*Δ::Cn *SP1* strains were grown on YPD media and suspended in PBS to an A_{600} of 0.1. Five 5-fold dilutions of each strain were spotted on YPD agar plates, incubated in 37 °C, and observed for 48 h. *B*, WT, Cn *sp1*Δ, *pkc1*Δ, Cn *sp1*Δ:Cn *SP1*, *pkc1*Δ::pACT-Cn *SP1*, and Cn *sp1*Δ::pACT-*PKC1* strains were grown on YPD plus sorbitol media, stained with India ink, and observed under microscopy. *C*, laccase activity. The above strains were plated following glucose starvation on asparagine plus neuroepinephrine media and incubated overnight. *D*, virulence of WT (*H99*), Cn *sp1*Δ, and Cn *sp1*Δ::Cn *SP1* strains was evaluated in a mice model following intravenous injection of 10^6 cfu. *, $p < 0.01$ for WT *versus* Cn *sp1*Δ and Cn *sp1*Δ::Cn *SP1 versus* Cn *sp1*Δ; $p > 0.05$ for WT *versus* Cn *sp1*Δ::Cn *SP1*.

a canonical zinc finger motif. It is not known whether this region in *S. cerevisiae* plays a role in DNA binding, although recent studies suggest the importance of three zinc motifs in DNA binding (42). Nevertheless, these studies demonstrate an evolutionary divergence between the cryptococcal Sp1 and the ascomycete Crz1.

*A Cn sp1*Δ *Mutant Shares Virulence Factor and Cell Wall Defects with a Cryptococcal pkc1*Δ *Mutant*—To establish a correlation between Cn *SP1* and the *PKC1* pathways, we compared phenotypic features of the two mutants, which showed a number of qualitative similarities. Both mutants had similar glossy-shiny colony morphologies under non-inducing conditions, due to subtly increased capsule production, as previously demonstrated by the same method for the *pkc1*Δ strain (16) (supplemental Fig. S6). India ink microscopy (Fig. 3*B*) of the two strains under the same conditions also demonstrated a shared increased capsule production in both, although the effect from the Cn *sp1*Δ mutation was more pronounced. Both mutants also shared decreased laccase production (Fig. 3*C*), which was more profound in the *pkc1*Δ mutant. Importantly, Cn *sp1*Δ exhibited attenuated virulence in a mouse model, showing the capacity for Cn *SP1* to mediate *PKC1*-mediated effects on virulence (Fig. 3*D*). Although not explicitly tested for virulence in previous reports (16), the cryptococcal *pkc1*Δ mutant would be expected to be avirulent, based on its inability to grow at 37 °C. Both mutants also exhibited cell wall/membrane dysfunction, manifested by sensitivity to cations and cell wall inhibitors as well as to the nitrosative agent $NaNO_2$ (Fig. 4 and Table 1). We also tested susceptibility of the strains to the pharmaceutical cell wall agent caspofungin, which showed that the Cn *sp1*Δ mutant displayed an intermediate sensitivity by MIC between WT and the *pkc1*Δ strains (WT, Cn *sp1*Δ::Cn *SP1*, and *pkc1*Δ::*PKC1*, 8 mg/ml; Cn *sp1*Δ, 4 mg/ml; and *pkc1*Δ, 0.25 mg/ml), suggesting a role for Cn *SP1* in resistance to this cell wall-active antifungal agent. In summary, cell wall dysfunction was more profound in the *pkc1*Δ strain in comparison with the Cn *sp1*Δ mutant, suggesting that Cn Sp1 may partially mediate a subset of *PKC1*-dependent phenotypes. However, unlike the *pkc1*Δ strain, Cn *sp1*Δ did not have a growth restriction at 37 °C with sorbitol or 30 °C in the absence of sorbitol (Figs. 3*A* and 4), suggesting no contribution of Cn Sp1 to these *PKC1*-dependent phenotypes.

*Overexpression of Cn SP1 Partially Restores Cell Wall Integrity Defects in a Cryptococcal pkc1*Δ *Mutant Strain*—To examine epistatic relationships between *PKC1* and Cn *SP1*, plasmids expressing each gene under the actin promoter were constructed and transformed into the other respective mutant, and overexpression was confirmed by quantitative PCR (normalized expression ± S.D.): Cn *SP1* expression in *pkc1*Δ::pACT-Cn *SP1*/*pkc1*Δ, 2.5 ± 0.5; *PKC1* expression in Cn *sp1*Δ::pACT-*PKC1*/Cn *sp1*Δ, 4.3 ± 1.6. Lack of *PKC1* expression in the *pkc1*Δ::pACT-Cn *SP1* strain was also confirmed by reverse

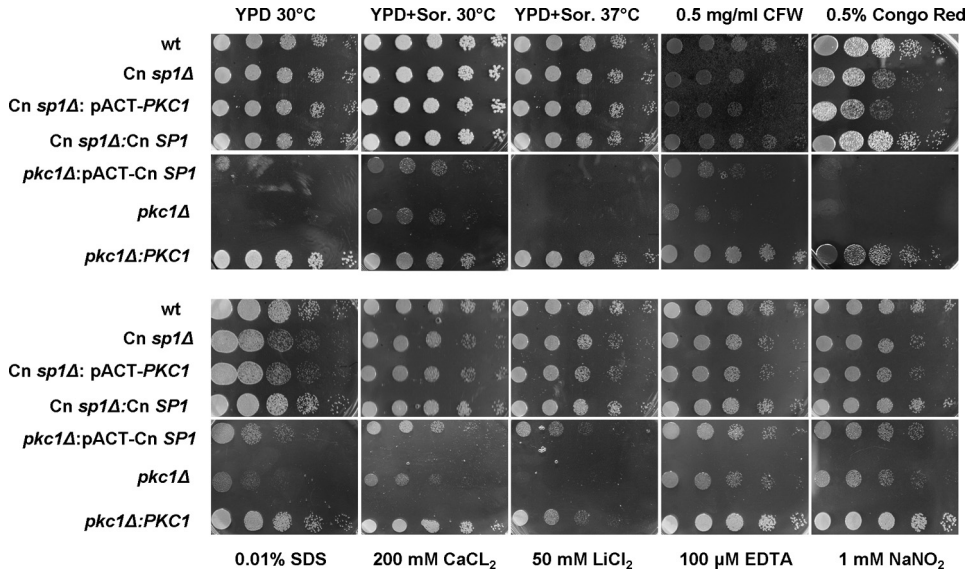

FIGURE 4. **Cn *sp1*Δ and *pkc1*Δ share cell wall integrity defects.** WT (*H99*), Cn *sp1*Δ, *pkc1*Δ, Cn *sp1*Δ::Cn *SP1*, *pkc1*Δ::*PKC1*, *pkc1*Δ::pACT-Cn *SP1*, and Cn *sp1*Δ::pACT-*PKC1* strains were grown on YPD plus sorbitol media and suspended in PBS medium to an A_{600} of 0.1. Five 5-fold dilutions of each strain were spotted on YPD plus 1 M sorbitol agar plates with the various additives as described and incubated at 30 °C (except for the 37 °C experiment) for 48 h. *CFW*, calcofluor white.

TABLE 1

Constituent expression of Cn *SP1* partially restores cell wall integrity in *pkc1*Δ

Phenotype is a comparison with wild type.

Strain	Temperature sensitivity (37°C)	India ink/ colony morphology	Melanin production	$NaNO_2$ sensitivity	Cell wall inhibitor sensitivity[1]	Capofungin sensitivity	Cation sensitivity[2]
Cn *sp1Δ*	wt	Hyper capsular/ mucoid	Moderately decreased	Moderate	Moderate	Profound	Moderate
Cn *sp1Δ:* pACT-*PKC1*	wt	Hyper capsular/ mucoid	Moderately decreased	Moderate	Moderate	Profound	Moderate
pkc1Δ	Profound	Aberrant/ mucoid	Profoundly decreased	Profound	Profound	Profound	Profound
pkc1Δ: pACT- Cn *SP1*	Profound	Aberrant/ dry, closer to wt	Profoundly decreased	Moderate	Moderate	Profound	Moderate

[1] Sensitivity to 0.01% SDS, 0.5% Congo red, and 0.5 mg/ml calcofluor white.
[2] Sensitivity to 200 mM $CaCl_2$ and 50 mM $LiCl_2$.

transcription PCR (data not shown). The *pkc1*Δ::pACT-Cn *SP1* strain demonstrated partially restored cell wall integrity (Fig. 4 and Table 1) in YPD without sorbitol as well as in YPD/sorbitol containing calcofluor white, SDS, $CaCL_2$, $LiCl_2$, and $NaNO_2$ (Fig. 4). *SP1* overexpression in the *pkc1*Δ mutant also partially restored the "dry" appearance of plated colonies (supplemental Fig. S6) and successfully restored the WT repressed capsule phenotype (Fig. 3*B*). Features that were not restored in the Cn *SP1*-overexpressing strain compared with the *pkc1*Δ strain were growth in 37 °C and in YPD/sorbitol with Congo red (Fig. 4), laccase expression (Fig. 2), and a reduced caspofungin MIC, which remained at 0.25. In contrast, overexpression of *PKC1* in the Cn *sp1*Δ mutant did not alter any growth, capsule, or cell wall phenotypes, including caspofungin sensitivity. These results support the hypothesis that Cn *SP1* acts downstream to *PKC1*, regulating a subpopulation of cell wall integrity functions.

Regulation of Cn SP1—We next sought to study the effect of glucose starvation on Cn Sp1 because a recently described role for autophagy suggests that nutrient deprivation plays an important role during cryptococcal infection (20), and laccase is known to be derepressed in the absence of glucose (43). In addition, because of the possible role of Cn Sp1 in the Pkc1 pathway, we studied conditions shown previously to be Pkc1-dependent: calcofluor white and $NaNO_2$ (16). As shown in Fig. 5*A*, Cn *SP1* transcription is induced under glucose starvation and was found to be dependent on an intact *PKC1* locus. During induction with calcofluor white and $NaNO_2$, Cn *SP1* transcript levels remained steady or were slightly reduced (Figs. 5, *B* and *C*, respectively) and were higher in the *pkc1*Δ compared with WT. Second, because *PKC1* is known to regulate the activity of transcription factors by phosphorylation, we analyzed for this by immunoprecipitating an N-terminally c-*myc*-tagged Cn Sp1 in a Cn *sp1*Δ background (Cn *sp1*Δ::pACT-Cn *SP1*) (Fig. 5*D*), followed by Western blotting using an anti-phosphoserine/threonine/tyrosine antibody (Fig. 5*E*). Interestingly, the Pkc1-inducing conditions, calcofluor white and $NaNO_2$, led to an increase in the phosphorylation of Cn Sp1, whereas there was no increase in phosphorylation under glucose starvation, suggesting complementary transcriptional and post-translational regulation of Cn Sp1 by Pkc1. Next, we studied the effect of these three conditions on the localization of GFP-Cn Sp1. As shown in Fig. 5*F*, a subset of the Cn Sp1 protein fraction is constitutively present in the nucleus, even under mid-log growth conditions in YPD. However, nuclear fractional localization of Cn Sp1 was increased during induction with calcofluor white and $NaNO_2$ but not after glucose starvation (Fig. 5, *F* and *G*), again suggesting both transcriptional and post-translational regulation by Pkc1. Both mechanisms would be expected to result in an increase in the total nuclear quota of the Cn Sp1 protein under all three inducing conditions by this combination of mechanisms, resulting in successful Pkc1-dependent signaling through Cn Sp1.

Cn SP1 and PKC1 Mediate a Similar Transcriptional Response to Glucose Starvation—We next conducted additional whole-genome epistatic experiments of Cn *SP1* and

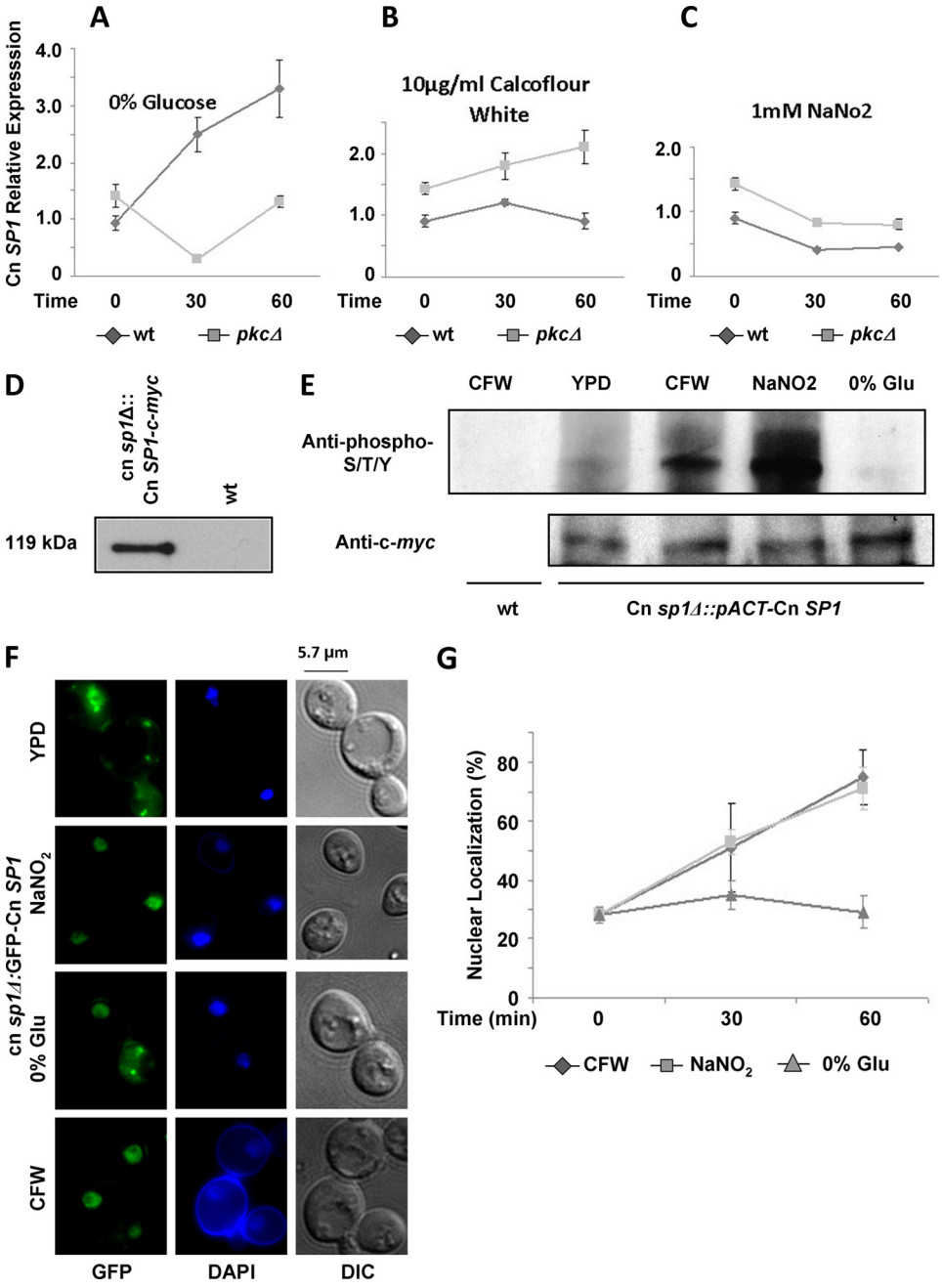

FIGURE 5. **Cn Sp1 is regulated by Pkc1.** *A–C*, Cn *SP1* expression was assayed in WT and *pkc1*Δ strains, before (mid-log phase in YPD medium) and following the detailed conditions by quantitative RT-PCR. Relative expression was calculated using *ACT1* as a reference gene. *D*, c-*myc*-tagged Cn Sp1 (Cn *sp1*Δ::pACT-Cn *SP1*) and WT strains were grown to mid-log phase in YPD and subjected to immunoprecipitation with anti c-*myc* antibody followed by Western blotting with anti c-*myc* Ab. *E*, Cn *sp1*Δ::pACT-Cn *SP1* cells were grown to mid-log phase and immunoprecipitated following a 1-h induction in medium under the indicated conditions (detailed under "Experimental Procedures"). Western blotting was done with either anti-phosphorylated Thr/Ser/Tyr or anti-c-*myc* as a loading control. Immunoprecipitated WT cells were used as a negative control. *F*, Cn *sp1*Δ::GFP-Cn *SP1* strains were grown to mid-log phase and induced for 1 h in medium under the indicated conditions (detailed under "Experimental Procedures"). Representative pictures of Cn *sp1*Δ::GFP-Cn *SP1* cells before and following 1-h induction are presented. DAPI was used for nuclear co-staining. *G*, percentage of nuclear localization of GFP-Cn *SP1* before and after 30 and 60 min of induction ($n = 300$ cells). *CFW*, calcofluor white; DIC, differential interference contrast.

PKC1 under starvation using microarray analysis (see "Experimental Procedures"). Fig. 6*a* shows a *y versus x* plot, whereby *y* describes transcript level changes of the Cn *sp1*Δ mutant compared with that of the wild type under starvation conditions, and *x* describes transcriptional differences between the *pkc1*Δ mutant and wild type, all under starvation conditions. The finding of a significant correlation in both direction and expression levels between the Cn *sp1*Δ and the *pkc1*Δ mutants (slope of $y = \log_2$(Cn *sp1*Δ/WT) *versus* $\log_2$(*pkc1*Δ/wt): 0.5907 ± 0.01; $p < 0.0001$) suggests a genetic relationship between the two genes, whereby genes down-regulated in the first mutant also tended to be down-regulated in the second. Using these plots, we first identified genes that were significantly down-regulated in both the *pkc1*Δ and Cn *sp1*Δ strains with a false discovery rate of <0.05 (Fig. 6*A*, *red* and *green dots*). From these, we selected the genes that were down-regulated by at least 2-fold (Fig. 6*A*, *green*

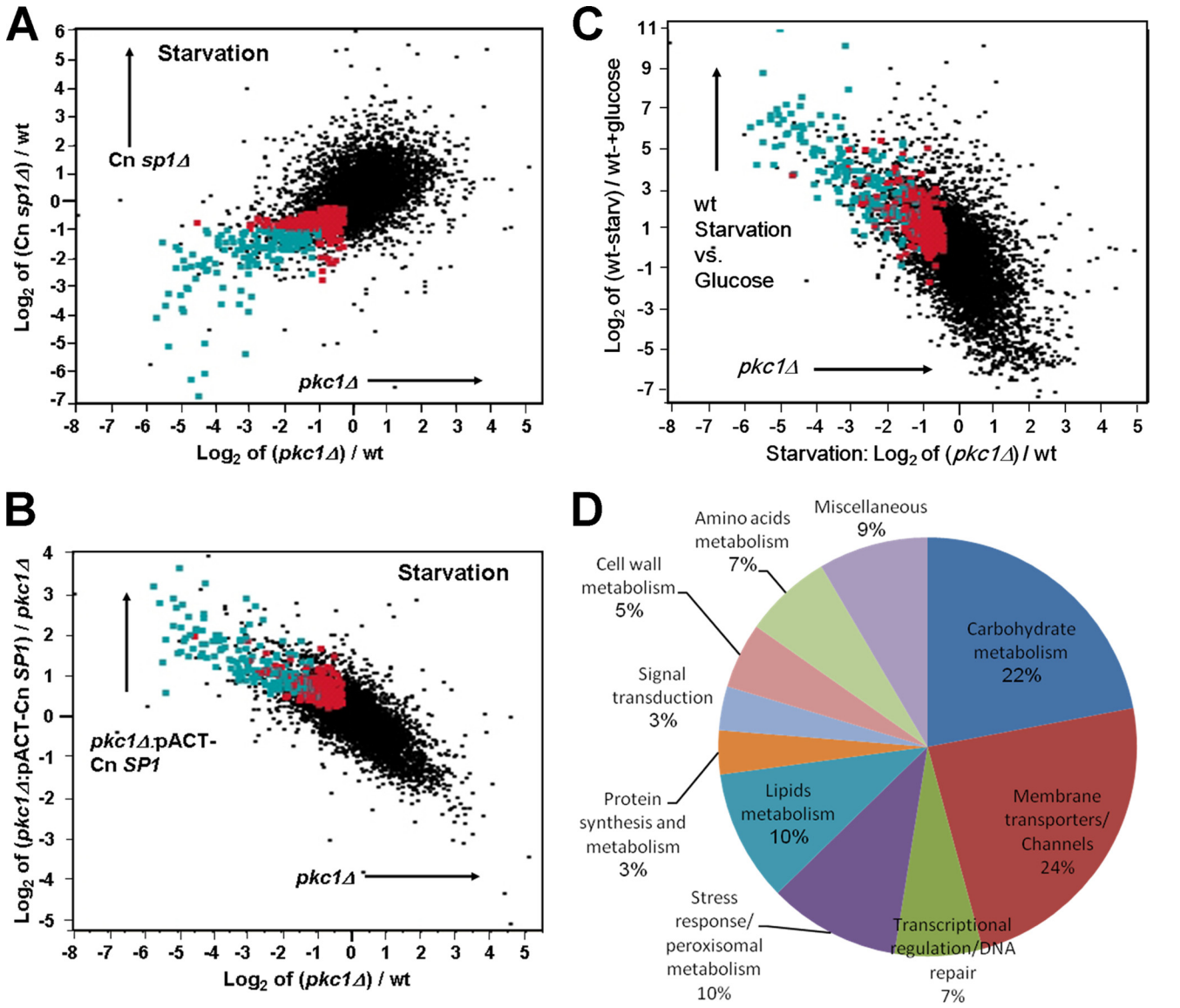

FIGURE 6. **The Cn Sp1/Pkc1 pathway regulates gene expression following glucose starvation.** *A*, transcriptional profile of Cn *sp1*Δ (*y* axis) and *pkc1*Δ (*x* axis) compared with WT following glucose starvation. *Red dots*, genes that are significantly down-regulated in Cn *sp1*Δ and *pkc1*Δ (false discovery rate <0.05) compared with WT. *Green dots*, a subset of the genes labeled in *red* that are also down-regulated by at least 2-fold compared with WT ($n = 163$). The genes in these groups are also presented in subsequent *panels*. *B*, transcriptional profile of *pkc1*Δ::pACT-Cn *SP1* (compared with *pkc1*Δ) and *pkc1*Δ (compared with WT) following glucose starvation, presented on the *y* and *x* axis, respectively. *Green* and *red*, the same transcripts as in *A*. *C*, transcriptional profile of WT (pre- and poststarvation) and *pkc1*Δ (compared with WT in starvation) presented on the *y* and *x* axis, respectively. *Green* and *red*, the same transcripts as in *A*. *D*, *pie diagram* detailing the functional categories of 59 genes with known function of the 163 genes identified in *A* (*green dots*).

dots). Of the 6970 genes tested in the microarray, 163 met both criteria (Table 2). Consistent with these results, overexpression of Cn *SP1* in the *pkc1*Δ mutant (*pkc1*Δ::pACT-Cn *SP1*) restored expression of a large majority of these genes, either completely or partially (>2-fold compared with *pkc1*Δ) in 102 genes (Fig. 6*C* and Table 2). Analysis of the entire transcriptome also showed a significant restoration of *PKC1*-dependent gene expression levels after Cn *SP1* overexpression as evidenced by a reversal of the slope of Fig. 6*B* *versus* that of Fig. 6*A* and *a* regression having a significant negative slope (slope of $y = \log_2(pkc1\Delta$::pACT-Cn *SP1*/*pkc1*Δ) *versus* $\log_2(pkc1\Delta/\mathrm{WT})$: -0.495 ± 0.005; $p < 0.0001$). Interestingly, careful comparison of the transcriptional profiles of the *sp1*Δ strain (Fig. 6*A*) with that of the *SP1* overexpressor strain (Fig. 6*C*) identified numerous genes (shown in *black*) that were scored as non-significant but showed significant up-regulation after *SP1* overexpression. One such gene, *HSP12*, was confirmed by Northern blot analysis to show reduced transcription in the *sp1*Δ mutant that was restored after *SP1* overexpression (supplemental Fig. S4*a*). This reflects the relatively conservative nature of the false discovery methodology commonly used for determining significance in transcriptional differences and shows the utility of whole genome epistatic studies in improving the efficiency of gene discovery in microarray experiments. Hsp12 has been recently found to display cAMP-dependent gene transcription in fungal pathogens *Candida albicans* and *C. neoformans* and was found in the latter to have a role in polyene antifungal drug susceptibility (43, 44). Interestingly, the majority of the population of Cn *SP1*/*PKC1*-dependent genes (151 of 163) were also induced in the WT strain during transition from mid-log phase growth

TABLE 2

Cn Sp1/Pkc1-regulated genes

Shown is a summary of identifiable genes (n = 59) down-regulated in both Cn *sp1*Δ and *pkc1*Δ compared with WT under glucose starvation (>2-fold difference and false discovery rate of <0.05), divided by functional categories. -Fold change in expression is presented in $\log_2$. The-fold change in gene expression in *pkc1*Δ::pACT-Cn *SP1* strain compared with *pkc1*Δ is also presented.

	Gene name	Cn *sp1Δ* *pkc1Δ* vs. wt		*pkc1Δ*:pACT-Cn *SP1* vs. *pkc1Δ*
Carbohydrate metabolism				
CNAG_05723	Alcohol dehydrogenase	-3.85	-3.01	2.89
CNAG_03785	α,α-trehalase	-1.25	-1.42	1.95
CNAG_02182	D-lactaldehyde dehydrogenase	-3.01	-4.74	1.81
CNAG_06672	Formate dehydrogenase	-3.27	-5.00	1.76
CNAG_00984	Glucose and ribitol dehydrogenase protein	-3.05	-3.36	1.41
CNAG_06374	Malate dehydrogenase	-1.95	-2.96	1.31
CNAG_04744	Mannose-6-phosphate isomerase	-1.57	-3.47	1.25
CNAG_02230	Phosphoketolase	-1.91	-3.36	1.17
CNAG_06169	R,R	-1.64	-2.51	0.87
CNAG_02000	Short-chain dehydrogenase	-2.80	-3.48	0.84
CNAG_03040	Transketolase	-1.31	-1.44	0.62
CNAG_00866	Transketolase	-2.27	-3.25	0.87
CNAG_02834	UDP-glucose:sterol glucosyltransferase	-1.42	-1.52	0.66
Membrane transporters/cnannels				
CNAG_04338	Cation diffusion facilitator 1	-1.08	-1.83	1.00
CNAG_06204	High-affinity nicotinic acid transporter	-1.66	-1.18	1.36
CNAG_01588	Hypothetical protein	-1.60	-2.63	1.73
CNAG_04416	Major facilitator superfamily transporter	-1.66	-2.09	0.78
CNAG_03502	Manganese resistance protein MNR2	-1.45	-2.26	1.04
CNAG_00905	MFS transporter	-1.03	-3.62	1.68
CNAG_01690	MFS transporter	-2.32	-5.10	2.22
CNAG_02527	Multidrug transporter	-1.71	-2.36	1.12
CNAG_05994	Multidrug transporter	-1.98	-3.15	1.38
CNAG_03824	Phosphate transport protein MIR1	-1.04	-2.31	1.00
CNAG_03432	Solute carrier family 2	-1.22	-1.52	0.61
CNAG_07874	Sugar transporter	-3.66	-5.44	1.33
CNAG_01742	Water channel	-2.30	-4.68	1.46
CNAG_04098	Xenobiotic-transporting ATPase	-1.59	-3.00	1.90
Stress response/peroxisomal metabolism				
CNAG_00575	Catalase 3	-2.99	-4.82	1.83
CNAG_04981	Catalase A	-1.44	-3.90	1.85
CNAG_01846	Flavoprotein	-1.71	-2.32	0.74
CNAG_02996	Flavoprotein oxygenase	-2.34	-2.19	0.84
CNAG_00315	HHE domain-containing protein	-2.45	-4.23	2.50
CNAG_03525	Trehalase	-1.72	-5.04	2.64
Lipids metabolism				
CNAG_03555	Acylglycerone-phosphate reductase	-2.16	-2.74	1.12
CNAG_02417	Lipase/esterase family protein	-1.46	-3.47	1.17
CNAG_07338	N-acyl-phosphatidylethanolamine-hydrolyzing phospholipase D	-1.39	-2.02	0.86
CNAG_04314	NAD+ kinase	-1.29	-3.51	1.39
CNAG_06594	Oxysterol binding protein	-1.07	-1.05	0.45
CNAG_04687	Stearoyl-CoA 9-desaturase	-1.37	-2.75	2.70
Amino acids metabolism				
CNAG_04417	2,4-dichlorophenoxyacetate alpha-ketoglutarate dioxygenase	-1.14	-4.19	3.25
CNAG_01912	Glutamine-dependent NAD(+) synthetase synthase	-1.24	-1.85	0.84
CNAG_00834	Phosphatidylserine decarboxylase	-2.50	-3.92	1.47
CNAG_06267	Rds1 protein	-1.62	-5.10	2.87
Transcriptional regulation/DNA repair				
CNAG_06602	Cysteine-type peptidase	-1.60	-2.77	0.97
CNAG_02690	Pirin	-1.47	-1.50	0.64
CNAG_05447	Pof4 protein	-1.23	-2.16	1.12
CNAG_05173	DNA-3-methyladenine glycosidase	-1.07	-1.65	0.58
Cell wall metabolism				
CNAG_06291	Deacetylase	-5.34	-3.11	2.09
CNAG_03771	DNA binding protein Ncp1	-1.41	-3.22	1.60
CNAG_05138	Exo-beta-1,3-glucanase	-1.28	-1.30	1.06
Protein synthesis and metabolism				
CNAG_05155	Protein-tyrosine-phosphatase	-2.07	-2.32	0.73
CNAG_02444	UPF0103 protein	-1.15	-2.09	1.08
Sulfur metabolism				
CNAG_04043	DUF636 domain-containing protein	-2.53	-3.01	1.10
CNAG_04206	DUF636 domain-containing protein	-2.08	-3.01	0.87
Miscellaneous				
CNAG_07800	Rop	-1.02	-1.06	0.44
CNAG_00254	NADH dehydrogenase	-1.09	-3.20	1.82
CNAG_07765	Bli-3 protein	-3.22	-5.33	1.88

to starvation conditions (Fig. 6*C*), suggesting an important role for the *PKC1*-Cn *SP1* pathway during nutrient stress.

Table 2 details genes that were down-regulated >2-fold with a false discovery rate of <0.05 in both *pkc1*Δ and Cn *sp1*Δ following glucose starvation. Functionally, these genes include those involved in carbohydrate metabolism, membrane transporters and channels, and general stress response (for an overview, see Fig. 6*D*). Genes involved in several virulence pathways were identified, including the *NTH1* gene involved in trehalose metabolism (45) and the allergen 1 gene involved in mucoid switch variants of *C. neoformans* (46). We validated the results presented in Table 2 and Fig. 6 by confirmation of a subset of genes by either Northern blot (supplemental Fig. S4*a*) or quantitative RT-PCR (supplemental Fig. S4*b*). We also confirmed several additional genes of interest that were found to be down-regulated in the mutants but had not met the statistical criteria similar to those of *HSP12* described above (supplemental Fig. S4). For example, expression of 1,3-β-glucan synthase, a target of the antifungal caspofungin (47) and a critical cell wall synthesis enzyme in *C. neoformans* (48), is increased following starvation in WT but decreased in *pkc1*Δ and Cn *sp1*Δ. WT expression is partially restored in the *pkc1*Δ::pACT-Cn *SP1* strain. This reduction may partially explain the increased susceptibility to caspofungin of both the Cn *sp1*Δ and the *pkc1*Δ mutants. However, the lack of restoration of caspofungin resistance in the *pkc1*Δ mutant by Cn Sp1 described above supports a role for additional genes in this unique cryptococcal resistance besides 1,3-β-glucan synthase expression, as suggested recently (49). The transcription of laccase was also reduced in the Cn *sp1*Δ but not in *pkc1*Δ (Fig. S4), despite reduced enzymatic activity in both (Fig. 3*C*), suggesting a complexity of regulation of this gene involving both transcriptional and post-transcriptional mechanisms.

Cn Sp1 Binds to Promoter Regions of Cn Sp1/Pkc1-dependent Genes—ChIP was performed using the Cn *sp1*Δ::pACT-Cn *SP1* strain, which expresses Cn Sp1 as a fusion with a c-*myc* affinity tag (see "Experimental Procedures"). Immunoprecipitation was performed using either an anti-c-*myc* monoclonal antibody (Ab) or a mouse IgG1 isotype control Ab, and promoter occupancy was quantified using a quantitative PCR assay. Promoter occupancy was expressed as a ratio of the target promoter signal immunoprecipitated by the c-*myc* antibody *versus* the iso-

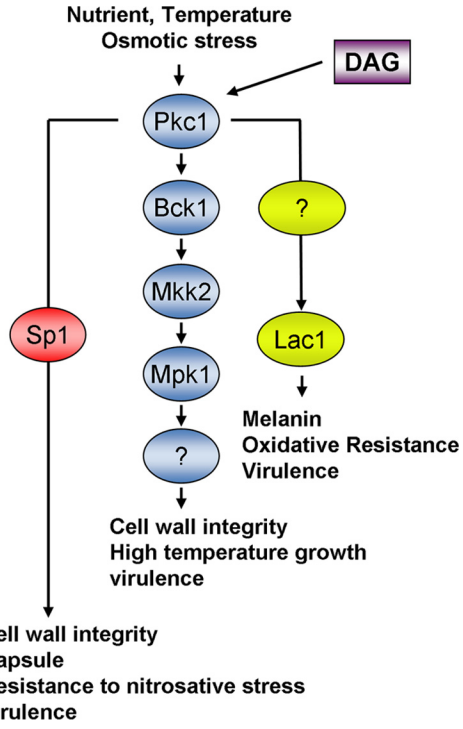

FIGURE 7. **Role of Sp1 in the Pkc1 signaling pathway of *C. neoformans*.** Pkc1 phosphorylates a member of the MAPK signaling pathway, Bck1, with subsequent phosphorylation of Mkk2 and the downstream component Mpk1 to mediate cell wall integrity, growth at high temperature, and virulence. Pkc1 also regulates the transcription factor Sp1 by phosphorylation, leading to activation by nuclear translocation as well as by transcriptional mechanisms, leading to regulation of osmoresistance, cell wall integrity, and virulence in parallel with the MAPK pathway as well as a unique pathway leading to resistance to nitrosative stress, capsule production, and caspofungin resistance. Laccase (Lac1) is regulated by Pkc1 via an unknown pathway. DAG, diacylglycerol. Adapted from Gerik *et al.* (16).

type control. Following glucose starvation, promoters of *HSP12* and *MDH* (malate dehydrogenase) showed increased promoter occupancy ratios of 230 ± 5.9 and 295.4 ± 37.4, respectively, whereas in mid-log phase cells, Cn Sp1 occupancy was increased for the *MDH* but not the *HSP12* promoters (29.7 ± 4.5 *versus* 0.61 ± 0.09, respectively). In contrast, DNA encoding the unrelated actin gene showed no enrichment after c-*myc* immunoprecipitation (data not shown). Furthermore, during starvation, the ratio of 1,4-α-glucan branching enzyme promoter to actin was 1.4 ± 0.34, and target gene signals were undetectable in mid-log phase cells, suggesting that this gene is not a direct target of Cn Sp1.

DISCUSSION

Previous work demonstrated that cryptococcal virulence and laccase expression are dependent on activation of the protein kinase C pathway by diacylglycerol (50, 51). A multiple-component pathway emanates from *PKC1*: one mediated through the MAPK signaling members, Bck1, Mkk2, and Mpk1, responsible for growth at high temperature and cell wall integrity and an additional unknown pathway(s) responsible for laccase expression, capsule regulation, and nitrosative stress (17). The present work confirms the existence of an additional parallel pathway and identifies a novel Pkc1-dependent C-terminal zinc finger transcription factor in fungi (Fig. 7). The reliance of the TF on Pkc1 was suggested by a screen using a microarray-based transcriptional comparison with known signal transduction mutants. An association with Pkc1 was then confirmed by a series of biochemical and epistatic experiments. The cryptococcal transcription factor was named Cn Sp1 because it is homologous to the Sp1/KLF transcription factor family within metazoans that, like Cn Sp1, contains three C-terminal Cys2His2-type zinc finger motifs.

Interestingly, Cn Sp1 also bears sequence similarity to a group of ascomycete C-terminal transcription factors with closest homology, by a simple BLAST search, to the calcineurin-responsive zinc finger protein, Crz1, but these typically contain only two canonical C-terminal zinc finger motifs (Fig. 2). Calcineurin-dependent signaling is important in a number of cellular processes in *C. neoformans*, including growth at elevated temperature, virulence, and sexual development. Expression of the virulence factor laccase also appears to be dependent on calcineurin, as evidenced by a role in calcium-dependent expression mediated by the transcriptional co-activator, Ssa1, and by the dependence of Ssa1 on Crz1 in *S. cerevisiae* (52). However, our studies showed that mutants of the cryptococcal Cn Sp1 did not share phenotypes with that of the calcineurin mutant *cna1*Δ, did not display calcineurin-dependent size shifts on an SDS-polyacrylamide gel, and did not display calcium-dependent nuclear localization, typical of the calcineurin-dependent ascomycete factor. This led us to screen for other potential signal transduction pathways using a microarray comparison screening approach.

Analysis of the C-terminal zinc finger motifs of Cn Sp1 allowed an evolutionary comparison of similar proteins within both fungi and metazoans because this region is more highly conserved and is an important functional signature of both the Crz1 and Sp family of proteins (39, 40). These studies demonstrated a complex evolutionary divergence of the cryptococcal TF from that of ascomycetes, such as *S. cerevisiae*. For example, although the second cryptococcal zinc finger motif shares closest homology with the second of two zinc finger motifs of the ascomycete Crz1, the first displays closer similarity to that of the metazoan and plant Sp/KLF homologs. Examination of a third cryptococcal zinc finger motif shows that it superficially displays homology to a non-canonical zinc finger-like motif within the ascomycete factors that has not been described previously. Excluding the ascomycete site would again place the cryptococcal canonical zinc finger site closest to the metazoan canonical zinc finger motifs. However, retention of the cysteine- and histidine-containing ascomycete sequences during evolution suggests that this third non-canonical zinc finger-like motif may have retained function. Because recent structural studies suggest a role for the third zinc finger motifs in determining DNA sequence specificity and binding affinity (40, 52), this divergent ascomycete motif could play a role in differentiating the DNA sequences recognized between the mammalian and ascomycete TFs. Interestingly, analysis of promoter sequences from the *HSP12* and *MDH* genes that showed Cn Sp1 promoter occupancy by chromatin immunoprecipitation identified the presence of consensus Sp1 binding sites (Hsp12, ^{490}CCGCCC; MDH, ^{59}CCGCCC) but not consensus Crz1 binding sites, again suggesting greater similarity to the metazoan TF. However, more detailed promoter dissection studies

are required to confirm these findings. In addition, examination of the *C. neoformans* annotated database (Broad Institute Web site) identified two C-terminal zinc finger proteins (*CNAG_00039* and *CNAG_01014*) that contained the requisite two zinc finger motifs of Crz1, but these did not share strong homology with the Crz1 protein either by BLAST or ClustalW algorithms. This suggests an evolutionary loss of the primordial Crz1 gene product function in *C. neoformans*. Indeed, previous attempts to identify a Crz1 homolog in *C. neoformans* by a number of methods, including a multicopy suppressor screen of a cryptococcal calcineurin mutant, failed to identify functional homologs of Crz1 in *C. neoformans* (27).

Interestingly, the Sp/KLF class of metazoan transcription factors is regulated by a variety of signal pathways, including protein kinase homologs *PKCζ*, which have been best studied in mammalian systems (40). These C-terminal transcription factors are also regulated by phosphorylation, similar to the cryptococcal factor. The metazoan TFs also act as coactivators of multiple pathways, including Ras and phosphatidylinositol 3-kinase pathways, suggesting interesting precedents to examine for Cn Sp1 in the future. However, it is important to be cautious in extrapolating functions to the cryptococcal Sp1, based on the distant phylogenetic relationships involved. Additional structural studies will be needed to differentiate Cn Sp1 from the metazoan factors.

Although it is difficult to make precise comparisons of functionality, it appears that the evolutionary structural drift of the fungal C-terminal zinc finger protein from Crz1 to Cn Sp1 also resulted in changes in the types of cellular functions regulated by this factor as compared with that reported previously for Crz1 from *S. cerevisiae* (39). For example, although a variety of cell wall synthetic functions are regulated by both Crz1 (chitin synthase type I, 1,3-β-glucan synthesis regulator *RHO1*) and Cn Sp1 (1,3-β-glucan synthase), Cn Sp1 appears to have picked up additional target functions in carbohydrate metabolism, including trehalose regulation and amino acid metabolism (such as the Rds1 protein, homologs of which are involved in ubiquitin-binding degradative functions (53)). In addition, expression of degradative target genes of *CRZ1*, such as carboxypeptidase and *ATG5*, the latter involved in autophagy induction (54), appears to have been lost in the evolution toward a Pkc1-dependent factor. Such changes in the regulatory landscape may have optimized relationships between environmental signals and cellular outputs that resulted in its evolution to a mammalian pathogen. Indeed, the cryptococcal Sp1 factor was found to mediate several important Pkc1-dependent phenotypes peculiar to its role as a pathogen, including capsule regulation and resistance to nitrosative stress. Importantly, Cn Sp1 was required for wild-type virulence in a mouse model. However, although the Cn *sp1*Δ mutant was defective in laccase expression, epistatic studies did not show restoration of the *pkc1*Δ laccase defect after Cn *SP1* overexpression, suggesting a role for additional pathway(s) mediating Pkc1-dependent laccase expression. Interestingly, our microarray epistatic transcriptional studies suggest that a preponderance of Pkc1-mediated transcription is dependent on Cn Sp1 signaling under glucose depletion conditions. However, these data should not be interpreted as implicating Cn Sp1 in all Pkc1-mediated transcription as cross-talk, and the role of the parallel MAPK pathway may lead to less reliance on Cn Sp1 under other Pkc1-associated conditions, such as oxidative or nitrosative stress. Interestingly, the dependence of some genes, such as malate dehydrogenase, showed strong reliance on both Pkc1 and Cn Sp1 by Northern analysis, whereas glucan synthase showed less dependence, suggesting such a role for multiple interacting signals communicating with Cn Sp1. Examination of the microarray epistatic experiments appears to bear this out, with a large variation in both *PKC1* and Cn *SP1*-dependent expression levels across the *C. neoformans* transcriptome. Such data show the advantage of a consideration of the whole genome in determining the regulatory impact of components of a signal transduction pathway. Induction of the glucose starvation response by Pkc1/Cn Sp1 may be particularly important in cryptococcal infections where nutrient deficiency encountered in host macrophages and brain is suggested by a role for autophagy during pathogenesis (20). Nutrient stress, in combination with host oxidative and temperature stress, is a host environmental component against which the fungus must compete for successful infection. The ability of the organism to induce transcriptional programs during nutrient limitation, such as that mediated by Pkc1-Cn Sp1 modeled here, during starvation may be a key component in niches leading to low metabolic states, such as during latent infection, demonstrated in recent clinical studies showing long periods of time within the host between initial infection and manifestation of disease during HIV-mediated immune suppression (55).

Acknowledgments—We would like to acknowledge the kind help of S. Giles for help with the annotation of the H99 C. neoformans database.

REFERENCES

1. Bichile, L. S., Gokhale, Y. A., Sridhar, V., and Gill, N. H. (2001) *J. Assoc. Physicians India* **49,** 377–378
2. Sorrell, T. C., Chen, S. C. A., Phillips, P., and Marr, K. A. (2011) *Cryptococcus: From Human Pathogen to Model Yeast*, pp. 595–606, American Society for Microbiology Press, Washington, D.C.
3. French, N., Gray, K., Watera, C., Nakiyingi, J., Lugada, E., Moore, M., Lalloo, D., Whitworth, J. A., and Gilks, C. F. (2002) *AIDS* **16,** 1031–1038
4. Park, B. J., Wannemuehler, K. A., Marston, B. J., Govender, N., Pappas, P. G., and Chiller, T. M. (2009) *AIDS* **23,** 525–530
5. Odom, A., Muir, S., Lim, E., Toffaletti, D. L., Perfect, J., and Heitman, J. (1997) *EMBO J.* **16,** 2576–2589
6. Salas, S. D., Bennett, J. E., Kwon-Chung, K. J., Perfect, J. R., and Williamson, P. R. (1996) *J. Exp. Med.* **184,** 377–386
7. Chang, Y. C., and Kwon-Chung, K. J. (1994) *Mol. Cell. Biol.* **14,** 4912–4919
8. Chang, Y. C., Penoyer, L. A., and Kwon-Chung, K. J. (1996) *Infect. Immun.* **64,** 1977–1983
9. Chang, Y. C., and Kwon-Chung, K. J. (1998) *Infect. Immun.* **66,** 2230–2236
10. Perez, P., and Calonge, T. M. (2002) *J. Biochem.* **132,** 513–517
11. Jung, U. S., and Levin, D. E. (1999) *Mol. Microbiol.* **34,** 1049–1057
12. Jung, U. S., Sobering, A. K., Romeo, M. J., and Levin, D. E. (2002) *Mol. Microbiol.* **46,** 781–789
13. Watanabe, Y., Irie, K., and Matsumoto, K. (1995) *Mol. Cell. Biol.* **15,** 5740–5749
14. Watanabe, Y., Takaesu, G., Hagiwara, M., Irie, K., and Matsumoto, K. (1997) *Mol. Cell. Biol.* **17,** 2615–2623
15. Kim, K. Y., Truman, A. W., and Levin, D. E. (2008) *Mol. Cell. Biol.* **28,** 2579–2589
16. Gerik, K. J., Bhimireddy, S. R., Ryerse, J. S., Specht, C. A., and Lodge, J. K.

(2008) *Eukaryot. Cell* **7,** 1685–1698
17. Gerik, K. J., Donlin, M. J., Soto, C. E., Banks, A. M., Banks, I. R., Maligie, M. A., Selitrennikoff, C. P., and Lodge, J. K. (2005) *Mol. Microbiol.* **58,** 393–408
18. Zhang, S., Hacham, M., Panepinto, J., Hu, G., Shin, S., Zhu, X., and Williamson, P. R. (2006) *Mol. Microbiol.* **62,** 1090–1101
19. Waterman, S. R., Hacham, M., Panepinto, J., Hu, G., Shin, S., and Williamson, P. R. (2007) *Infect. Immun.* **75,** 714–722
20. Hu, G., Hacham, M., Waterman, S. R., Panepinto, J., Shin, S., Liu, X., Gibbons, J., Valyi-Nagy, T., Obara, K., Jaffe, H. A., Ohsumi, Y., and Williamson, P. R. (2008) *J. Clin. Invest.* **118,** 1186–1197
21. Cox, G. M., Toffaletti, D. L., and Perfect, J. R. (1996) *J. Med. Vet. Mycol.* **34,** 385–391
22. Edgar, R. C. (2004) *Nucleic Acids Res.* **32,** 1792–1797
23. Swofford, D. L. (2003) *PAUP*: Phylogenetic Analysis Using Parsimony (*and Other Methods)*, Version 4, Sinauer Associates, Sunderland, MA
24. Liu, X., Hu, G., Panepinto, J., and Williamson, P. R. (2006) *Mol. Microbiol.* **61,** 1132–1146
25. Liu, L., Tewari, R. P., and Williamson, P. R. (1999) *Infect. Immun.* **67,** 6034–6039
26. Park, Y. D., Panepinto, J., Shin, S., Larsen, P., Giles, S., and Williamson, P. R. (2010) *J. Biol. Chem.* **285,** 34746–34756
27. Kraus, P. R., Boily, M. J., Giles, S. S., Stajich, J. E., Allen, A., Cox, G. M., Dietrich, F. S., Perfect, J. R., and Heitman, J. (2004) *Eukaryot. Cell* **3,** 1249–1260
28. Benjamini, Y., and Hochberg, Y. (1995) *J. R. Stat. Soc. Ser. B* **57,** 289–300
29. Chow, E. D., Liu, O. W., O'Brien, S., and Madhani, H. D. (2007) *Curr. Genet.* **52,** 137–148
30. Ren, B., Robert, F., Wyrick, J. J., Aparicio, O., Jennings, E. G., Simon, I., Zeitlinger, J., Schreiber, J., Hannett, N., Kanin, E., Volkert, T. L., Wilson, C. J., Bell, S. P., and Young, R. A. (2000) *Science* **290,** 2306–2309
31. Zhu, X., Gibbons, J., Garcia-Rivera, J., Casadevall, A., and Williamson, P. R. (2001) *Infect. Immun.* **69,** 5589–5596
32. Boustany, L. M., and Cyert, M. S. (2002) *Genes Dev.* **16,** 608–619
33. Karababa, M., Valentino, E., Pardini, G., Coste, A. T., Bille, J., and Sanglard, D. (2006) *Mol. Microbiol.* **59,** 1429–1451
34. Yue, C., Cavallo, L. M., Alspaugh, J. A., Wang, P., Cox, G. M., Perfect, J. R., and Heitman, J. (1999) *Genetics* **153,** 1601–1615
35. Williamson, P. R. (1994) *J. Bacteriol.* **176,** 656–664
36. Rafty, L. A., and Khachigian, L. M. (2001) *Nucleic Acids Res.* **29,** 1027–1033
37. Cramer, T., Jüttner, S., Plath, T., Mergler, S., Seufferlein, T., Wang, T. C., Merchant, J., and Höcker, M. (2008) *Cell. Signal.* **20,** 60–72
38. Schultz, J., Milpetz, F., Bork, P., and Ponting, C. P. (1998) *Proc. Natl. Acad. Sci. U.S.A.* **95,** 5857–5864
39. Cyert, M. S. (2003) *Biochem. Biophys. Res. Commun.* **311,** 1143–1150
40. Wierstra, I. (2008) *Biochem. Biophys. Res. Commun.* **372,** 1–13
41. Klug, A., and Schwabe, J. W. (1995) *FASEB J.* **9,** 597–604
42. Lee, J., Kim, J., and Seok, C. (2010) *J. Phys. Chem. B* **114,** 7662–7671
43. Maeng, S., Ko, Y. J., Kim, G. B., Jung, K. W., Floyd, A., Heitman, J., and Bahn, Y. S. (2010) *Eukaryot. Cell* **9,** 360–378
44. Sheth, C. C., Mogensen, E. G., Fu, M. S., Blomfield, I. C., and Mühlschlegel, F. A. (2008) *Fungal Genet. Biol.* **45,** 1075–1080
45. Ngamskulrungroj, P., Himmelreich, U., Breger, J. A., Wilson, C., Chayakulkeeree, M., Krockenberger, M. B., Malik, R., Daniel, H. M., Toffaletti, D., Djordjevic, J. T., Mylonakis, E., Meyer, W., and Perfect, J. R. (2009) *Infect. Immun.* **77,** 4584–4596
46. Jain, N., Li, L., Hsueh, Y. P., Guerrero, A., Heitman, J., Goldman, D. L., and Fries, B. C. (2009) *Infect. Immun.* **77,** 128–140
47. Kartsonis, N. A., Nielsen, J., and Douglas, C. M. (2003) *Drug Resist. Updat.* **6,** 197–218
48. Thompson, J. R., Douglas, C. M., Li, W., Jue, C. K., Pramanik, B., Yuan, X., Rude, T. H., Toffaletti, D. L., Perfect, J. R., and Kurtz, M. (1999) *J. Bacteriol.* **181,** 444–453
49. Maligie, M. A., and Selitrennikoff, C. P. (2005) *Antimicrob. Agents Chemother.* **49,** 2851–2856
50. Heung, L. J., Luberto, C., Plowden, A., Hannun, Y. A., and Del Poeta, M. (2004) *J. Biol. Chem.* **279,** 21144–21153
51. Heung, L. J., Kaiser, A. E., Luberto, C., and Del Poeta, M. (2005) *J. Biol. Chem.* **280,** 28547–28555
52. Yoshimoto, H., Saltsman, K., Gasch, A. P., Li, H. X., Ogawa, N., Botstein, D., Brown, P. O., and Cyert, M. S. (2002) *J. Biol. Chem.* **277,** 31079–31088
53. Yashiroda, H., Kaida, D., Toh-e, A., and Kikuchi, Y. (1998) *Gene* **225,** 39–46
54. Yang, Z., and Klionsky, D. J. (2010) *Nat. Cell Biol.* **12,** 814–822
55. Dromer, F., Mathoulin, S., Dupont, B., and Laporte, A. (1996) *Clin. Infect. Dis.* **23,** 82–90